View metadata, citation and similar papers at core.ac.uk

brought to you by CORE

provided by Elsevier - Publisher Connector

Chloramine T-induced structural and biochemical changes in echistatin

C. Chandra Kumar[a,*], Huiming Nie[a], Lydia Armstrong[a], Rumin Zhang[a], Senadhi Vijay-Kumar[b], Anthony Tsarbopoulos[1,a]

[a] *Departments of Tumor Biology, Structural chemistry, Schering-Plough Research Institute, 2015, Galloping Hill Road, Kenilworth, NJ 07033, USA*
[b] *FELS Institute for Cancer Research and Molecular Biology, Temple University School Of Medicine, Philadelphia, PA 19140, USA*

Received 13 April 1998

Abstract Echistatin is a member of the disintegrin family of peptides and a potent inhibitor of platelet aggregation and cell adhesion. Echistatin binds to integrin $\alpha_v\beta_3$ and $\alpha_{IIb}\beta_3$ receptors with high affinity. Binding is mediated by an RGD-containing loop maintained in an appropriate conformation by disulfide bridges. In this study, we have compared the binding characteristics of echistatin iodinated by either lactoperoxidase or chloramine T method. We show that echistatin labeled by lactoperoxidase method binds to integrin $\alpha_v\beta_3$ receptor with high affinity and in a non-dissociable manner very similar to native echistatin. In contrast, chloramine T-labeled echistatin can rapidly dissociate from the receptor. We demonstrate that chloramine T reaction results in the addition of an extra oxygen to the methionine residue adjacent to the RGD motif in echistatin. Modeling studies and molecular dynamic simulation studies show that the extra oxygen atom on the methionine residue can form hydrogen bonds with the glycine and aspartic acid residues of the RGD motif. These structural changes in echistatin help explain the changes in the binding characteristics of the molecule following chloramine T reaction.

© 1998 Federation of European Biochemical Societies.

Key words: Echistatin; Integrin receptor; Chloramine T; Oxidation; RGD motif

1. Introduction

Echistatin is a 49 amino acid peptide derived from the venom of Echis carinatus and belongs to the disintegrin family of peptides [1,2]. So far about 30 disintegrins have been isolated and characterized from the venoms of many species of snakes [1–3]. These disintegrins contain 49–84 amino acids and 8–14 cysteine residues linked by intramolecular disulfide bonds [4–6]. The three-dimensional structure of echistatin has been determined in aqueous solution by nuclear magnetic resonance (NMR) spectroscopy [7]. The sequence of echistatin contains eight cysteine residues forming four disulfide bridges [1,8]. NMR-derived structure for echistatin reveals that the RGD sequence is present in a loop between two β strands of the protein protruding 14–17 Å from the protein core. The activity of echistatin depends on the appropriate pairing of eight cysteines by S-S bridges, which maintain RGD-containing loop in an appropriate conformation. Echistatin binds with high affinity to several integrins and is a potent inhibitor of platelet aggregation and cell adhesion.

Integrins are a family of structurally related heterodimeric cell surface receptors that mediate cell-cell and cell-matrix interactions [9–11]. Integrins bind to proteins present in the extracellular matrix and mediate anchorage and convey signals that regulate cell growth, differentiation and migration [11–13]. Many of the integrin receptors bind to a common recognition sequence, comprising arginine-glycine-aspartic acid (RGD) in the macromolecular ligands such as fibronectin, vitronectin, von Willebrand factor and fibrinogen [13]. The integrin $\alpha_v\beta_3$ is expressed on endothelial cells, smooth muscle cells, osteoclasts, melanoma and other cell types where it plays an important role in physiological processes that include angiogenesis and tissue repair, as well as pathological conditions such as osteoporosis, tumor cell metastasis and tumor-induced angiogenesis [14]. Recent results indicate a key role for this integrin in a signaling event critical for the survival and ultimate differentiation of vascular cells undergoing angiogenesis in vivo [14–16]. Echistatin is a more potent inhibitor of ligand binding to purified $\alpha_v\beta_3$ and $\alpha_5\beta_1$ than to purified $\alpha_{IIb}\beta_3$.

In this study, we show that echistatin radiolabeled with ^{125}I by chloramine T method shows strikingly different binding characteristics to integrin $\alpha_v\beta_3$ receptor compared to either native or lactoperoxidase-labeled ^{125}I-echistatin. Mass spectrometric analysis of the chloramine T-treated echistatin indicates the addition of an extra oxygen atom to the methionine residue adjacent to the RGD sequence. Modeling studies and molecular dynamic simulation studies show that the extra oxygen atom on the methionine residue can form hydrogen bonds with the glycine and aspartic acid residues of the RGD motif. These structural changes in echistatin account for the changes in the binding characteristics of the molecule.

2. Materials and methods

2.1. Materials

Synthetic RGD-containing peptides were purchased from Gibco-BRL (Gaithersburg, MD, USA). Octyl-β-D-glucopyranoside and Nonidet-P-40 were purchased from Sigma Chemical Company (St. Louis, MI, USA). Microlite-2 plates were obtained from Dynatech Corporation (Chantilly, VA, USA). $\alpha_v\beta_3$-specific (LM609) monoclonal antibodies and LM609 coupled to affigel matrix were purchased from Chemicon International Inc., (Temecula, CA, USA). ^{125}I-echistatin labeled by chloramine T method or by lactoperoxidase method to a specific activity of 2000 Ci/mmole were from Amersham International (Chicago, IL, USA). Echistatin was purchased from Bachem (Torrence, CA, USA).

2.2. Protein purification and solid phase receptor binding assay

$\alpha_v\beta_3$ was purified as described by Orlando and Cheresh [18]. The receptor binding assay was performed as described previously [17,18].

2.3. Peptide synthesis

The peptide fragments derived from echistatin (residue 20 to 32) were synthesized on an ABI 431A peptide synthesizer using Fmoc

*Corresponding author. Fax: +1 (908) 298-3918.
E-mail: Chandra.kumar@spcorp.com

[1]Current address: GAIA Research Center, The Goulandris Natural History Museum, 13 Levidou street, 145 62 Kifissia, Greece.

0014-5793/98/$19.00 © 1998 Federation of European Biochemical Societies. All rights reserved.
PII S0014-5793(98)00587-0

chemistry and an Fmoc Amide resin (Applied Biosystems, Foster City, CA, USA). The side chains of trifunctional residues were protected by tert-butyl (for Asp and Tyr), trityl (for Cys), tert-butyloxycarbonyl (for Lys), and 2,2,4,6,7-pentamethyldihydrobenzofuran-5-sulfonyl (for Arg). The peptides were cleaved and deprotected by concentrated trifluoroacetic acid (80% TFA) in the presence of scavengers (4% each of phenol, H_2O, thioanisole, ethanedithiol, and triisopropylsilane). The cleaved peptides were extracted into cold ethyl ether. The crude peptides were purified by reversed phase high performance liquid chromatography. The molecular masses of the purified peptides were confirmed by mass spectroscopy. Chloramine T and lactoperoxidase treatments of echistatin and peptides were carried out in the absence of NaI^{125} as suggested by the manufacturer (Amersham International, Chicago, IL, USA).

2.4. Mass spectrometry

Electrospray mass spectra were acquired on a Perkin-Elmer Sciex (Concord, Canada) API III triple-quadrupole mass spectrometer equipped with an atmospheric pressure ion source, kept at 60°C, and an ion-spray interface [19,20]. Echistatin and the CT-/LP-treated products were dissolved in 0.1% aqueous TFA to a concentration in the low mM range (ca.5 pmol/ml). The samples were then infused into the ion-spray source of the mass spectrometer at a flow rate of 5 ml/min for the duration of several full-scan spectra. The final spectrum was an averaged sum of several scans [21,22] from m/z 600 to 2000 (MCA mode) at a scan rate of 3 s/scan. The average molecular weight was derived from all the observed charge states with an accuracy of 1–2 Da from the expected mass.

Plasma desorption mass spectrometric analysis of the 13 amino acid synthetic echistatin peptides and their CT-/LP-treated products was performed using a BIOION 20 californium-252 time-of-flight mass spectrometer set at an acceleration voltage of 15 kV. The samples were dissolved in 2:1 (v/v) aqueous TFA/ethanol and spin-dried prior to their introduction into the source of the mass spectrometer [22].

2.5. Development of three-dimensional structure of chloramine T-labeled echistatin using homology methods

The three-dimensional structure of modified echistatin was built using the coordinates of echistatin determined experimentally using NMR methods [4]. The change in methionine residue was incorporated on ESV graphics system using FRODO package [23] and refined for stereochemistry optimization. The model was then energy-minimized using conjugate gradient minimizing method of Powell [24]. The energy-minimized structure of modified echistatin was further refined using molecular dynamics simulation methods using X-PLOR [25]. Comparison of 3D structures of echistatin and echistatin with methionine sulfoxide at position 28 showed that both the structures were very similar except for small local changes around methionine residue (Fig. 6). Various molecular dynamics protocols used for developing the structure of echistatin with methionine sulfoxide, and the searches for conformational space for global minima, converged to the same three-dimensional structure. The total energy of echistatin with methionine sulfoxide compared well with that of the native echistatin.

3. Results and discussion

3.1. Binding characteristics of lactoperoxidase and chloramine T-labeled ^{125}I-echistatin to purified $\alpha_v\beta_3$ receptor

Echistatin was radiolabeled with ^{125}I either by lactoperoxidase (LP) or chloramine T (CT) method and its binding to purified $\alpha_v\beta_3$ was measured using a solid phase receptor binding assay as described in Section 2 [17,26]. Incubation of purified $\alpha_v\beta_3$ (10 ng) with increasing concentrations of LP- or CT-labeled echistatin for 3 h resulted in a saturable and specific binding (Fig. 1). Non-specific binding was evaluated by carrying out the binding assay in the presence of 200-fold molar excess of echistatin and was typically less than 10 percent of the total binding. The data were analyzed by non-linear regression using graph-pad prism [17]. LP-labeled echistatin binds to $\alpha_v\beta_3$ with an apparent K_d of 0.3 nM, whereas

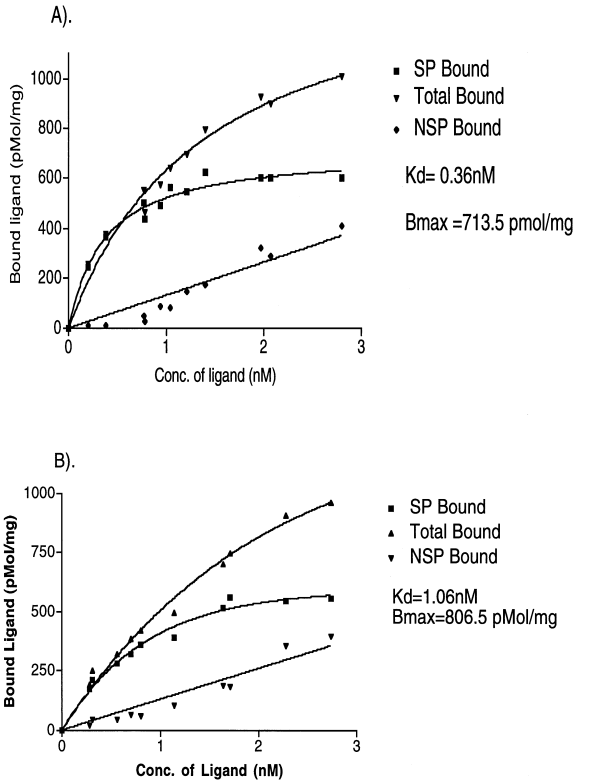

Fig. 1. Scatchard analysis of LP- or CT-labeled ^{125}I-echistatin binding to purified $\alpha_v\beta_3$ integrin receptor. Saturation binding isotherms of LP- (A) or CT- (B) labeled ^{125}I-echistatin binding to $\alpha_v\beta_3$ receptor were determined in a solid phase receptor binding assay as described in Section 2. Integrin $\alpha_v\beta_3$ purified from human placenta was coated at a concentration of 10 ng/well onto Microlite-2 plates and incubated with various concentrations (0.05–5 nM) of ^{125}I-echistatin for 3 h at room temperature. Bound ligand concentration was determined by solubilizing the counts with boiling 2 N NaOH and subjected to gamma counting. Non-specific binding was evaluated by carrying out the binding assay in the presence of 200-fold molar excess of cold echistatin and was subtracted from the total binding to calculate specific binding. Each data point is an average of triplicate measurements in which the error was less than 5% of the total binding. To derive the affinity of the interaction between echistatin and $\alpha_v\beta_3$, the data shown in panel A were analyzed by non-linear regression analysis using graph-pad prism program.

CT-labeled echistatin exhibited a K_d value of 1 nM (Fig. 1A and B). The B_{max} value for the binding reactions using the two ligands was 750 pmoles/mg protein. Scatchard analysis of the binding data using ligand computer program gave identical results. Thus CT-labeled echistatin has a slightly lower affinity for $\alpha_v\beta_3$ receptor compared to LP-labeled echistatin.

Next, we compared the K_i values for the various RGD peptides in competition type experiments using either LP- or CT-labeled echistatin. The concentrations required for half-maximal inhibition of the binding of LP-labeled echistatin to $\alpha_v\beta_3$ receptor were calculated to be 0.3 ± 0.06 nM for echistatin and 445 ± 102 nM and 183 ± 22 nM for linear RGD peptide and cyclic RGD peptide respectively (Fig. 2A). The corresponding values for CT-labeled echistatin were, 0.3 ± 0.06 nM for echistatin and 6 ± 0.7 nM and 1 ± 0.20 nM for linear and cyclic RGD peptide respectively (Fig. 2B). A linear hexamer peptide containing RGE sequence failed to compete for the binding of either LP- and CT-labeled echi-

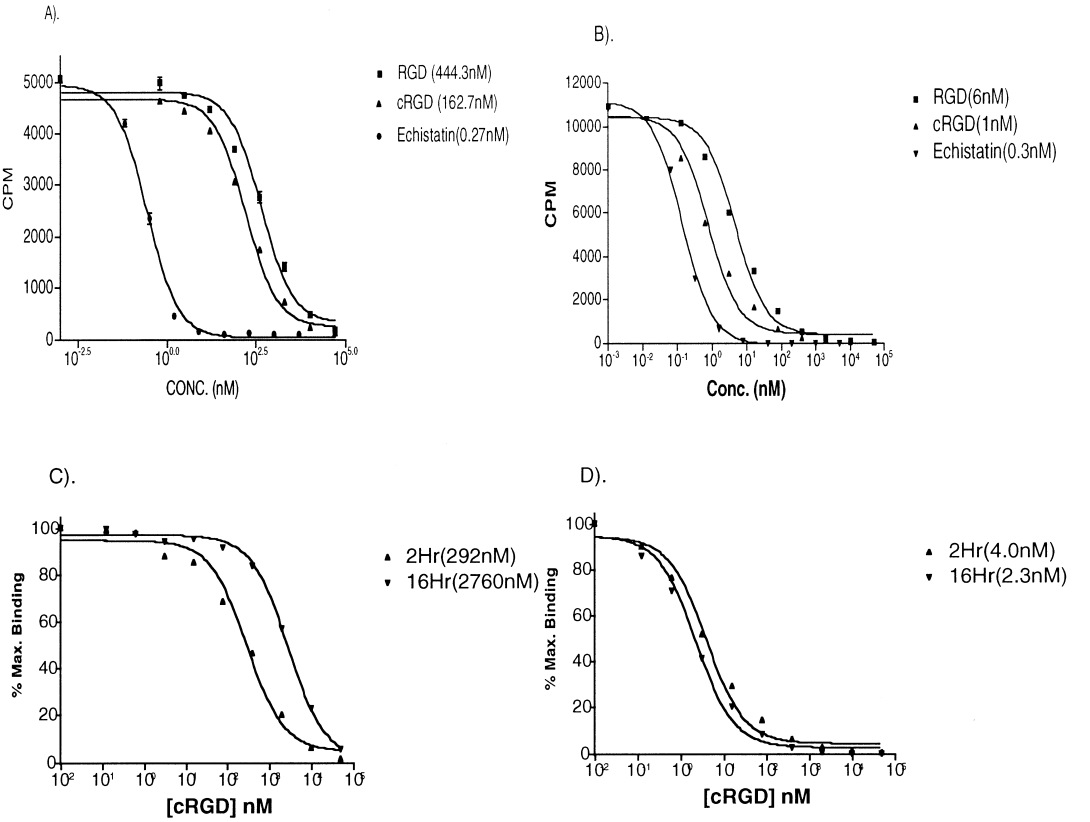

Fig. 2. Competition of RGD peptides for the binding of either LP- or CT-labeled echistatin to $\alpha_v\beta_3$ receptor. A: Purified receptor was coated onto Microlite-2 plates at a concentration of 50 ng/well as described above. LP- (A) or CT- (B) labeled ^{125}I-echistatin was added to the wells to a final concentration of 0.05 nM in binding buffer (50 μl/well) in the presence of different concentrations of the competing ligands. Cold unlabeled echistatin, GRGDSP, and Gpen RGDSp peptides dissolved in binding buffer at the concentrations indicated were added to the wells before the addition of radioligand. After a 3 h incubation at room temperature, the wells were washed thoroughly with binding buffer and radioactivity was determined using Top count (Packard). Effect of varying the incubation times of the receptor binding reactions on the concentrations of the various competitors required for half-maximal binding (C and D). LP- (C) or CT-labeled (D) ^{125}I-echistatin was incubated with $\alpha_v\beta_3$ receptor in the presence of various concentrations of peptides for 2 or 16 h, the wells were washed with binding buffer and radioactivity was determined using Top count (Packard). All measurements were done in triplicate with standard deviations less than 10%.

statin to $\alpha_v\beta_3$ receptor (data not shown). Even though LP- and CT-labeled ^{125}I-echistatin bind to integrin $\alpha_v\beta_3$ receptor with similar affinities, the concentrations of linear and cyclic RGD peptides required for half-maximal inhibition were strikingly different. Significantly higher concentrations of RGD peptides were required for competing the binding of LP-labeled echistatin to $\alpha_v\beta_3$ compared to CT-labeled echistatin. The K_i values for unlabeled echistatin in these competition experiments are identical for echistatin labeled by the two methods.

Next, we determined the effect of varying the incubation times of the binding reactions on the K_i values for linear and cRGD peptides using the two ligands. In these experiments, LP- or CT-labeled echistatin was incubated for different intervals of time with $\alpha_v\beta_3$ receptor in the presence of increasing concentrations of cRGD peptide and the amount of ligand bound to the receptor was determined in the solid phase receptor binding assay. As shown in Fig. 2C and D, the K_i values of cRGD peptide increased significantly with longer incubation times (2 h vs. 16 h), with LP-labeled echistatin. The concentrations of cRGD required to compete for half-maximal binding of LP-labeled echistatin to $\alpha_v\beta_3$ during a 2 h incubation period was 292 ± 68 nM and the corresponding value for 16 h incubation was 2760 ± 250 nM. However, the corresponding K_i values for the cRGD peptide using CT-labeled echistatin were 4 ± 1 nM (2 h) and 2.3 ± 0.45 nM (16 h) (Fig. 2D). Hence, higher concentrations of cRGD peptide were required to compete for the binding of LP-labeled echistatin to $\alpha_v\beta_3$ receptor compared to CT-labeled molecule and this value increased proportionally with longer incubation times for LP-labeled echistatin. In contrast, the concentrations of cRGD peptide required to compete for half-maximal binding of CT-labeled echistatin did not change dramatically with an increase in incubation time.

3.2. *Chloramine T-labeled ^{125}I-echistatin binds to $\alpha_v\beta_3$ receptor in a dissociable manner*

To understand the biochemical basis for the differences in the binding characteristics of LP- and CT-labeled echistatin, we determined the off-rate kinetics of the two ligands bound to $\alpha_v\beta_3$ receptor. In this experiment, LP- or CT-labeled ^{125}I-echistatin was incubated with $\alpha_v\beta_3$ receptor for 3 h, the unbound ligand was removed and the wells were washed with binding buffer followed by the addition of either binding buffer or increasing concentrations of unlabeled competitors. Under these conditions, LP-labeled ^{125}I-echistatin bound to the $\alpha_v\beta_3$ receptor showed very little dissociation in the presence of either cold echistatin or linear and cRGD peptides

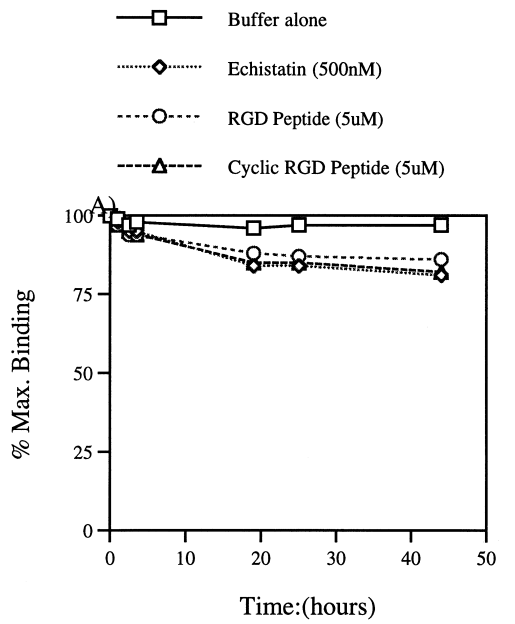

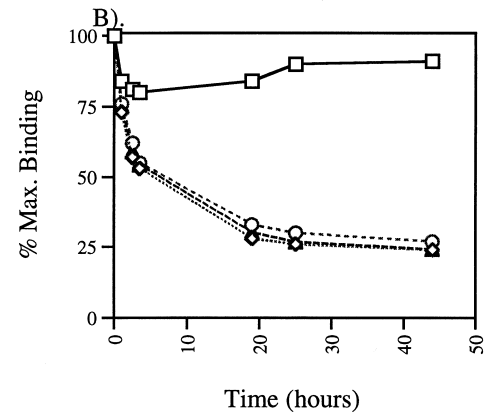

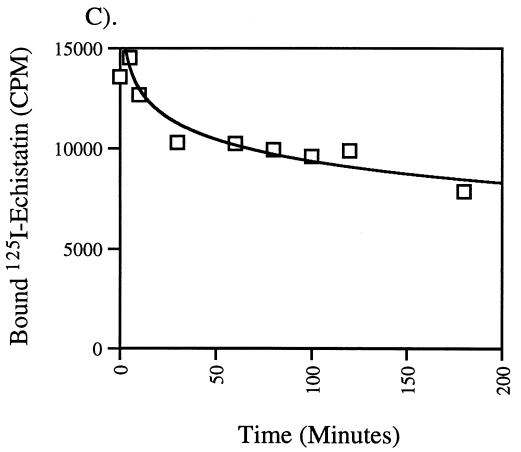

Fig. 3. Chloramine T-labeled ^{125}I-echistatin binds to $\alpha_v\beta_3$ receptor in a dissociable manner. A: The dissociability of the lactoperoxidase-labeled ^{125}I-echistatin was determined by preincubating the receptor with radiolabeled echistatin for 3 h and removing the unbound ligand, washing with binding buffer and then incubating with either buffer or 50 nM of cold echistatin or 500 nM of linear RGD, or 500 nM of cyclic RGD peptide for different times. The concentration of bound ligand was determined at various times as described in the legend to Fig. 1. The amount of labeled ligand bound to $\alpha_v\beta_3$ was given an arbitrary value of 100 percent. All points represent triplicate determinations with error of less than 5%. B: The experiment was repeated as described above using CT-labeled echistatin. C: Measurement of the dissociation kinetics of CT-labeled ^{125}I-echistatin from $\alpha_v\beta_3$. To determine the dissociation rate constant, CT-labeled ^{125}I-echistatin at 1 nM concentration was incubated with $\alpha_v\beta_3$ receptor coated onto 96-well Microlite-2 plates for 3 h at room temperature. The wells were washed thoroughly followed by the incubation of 100 μl/well of blocking/binding buffer. At the times indicated, the buffer was withdrawn and the wells were washed twice with binding buffer and the bound radioactivity was determined as described in the legend to Fig. 1. Non-specific binding was measured by the coincubation of excess echistatin peptide and represented 10 percent of the total binding. All points were the average of triplicates with error measurements of less than 5%.
←

(Fig. 3A), indicating that LP-labeled echistatin binds to $\alpha_v\beta_3$ in a non-dissociable manner. When the receptor was saturated with native unlabeled echistatin for 3 h before removing the unbound ligand and replaced with radiolabeled ligand, there was very little binding, suggesting that native echistatin also binds to $\alpha_v\beta_3$ receptor in a non-dissociable manner. In contrast, when CT-labeled echistatin was used in these experiments, unlabeled echistatin, linear and cRGD peptides were able to displace the bound ligand indicating that CT-labeled echistatin binds to $\alpha_v\beta_3$ receptor in a dissociable manner (Fig. 3B). Thus chloramine T reaction seemed to alter the protein in such a way that its interaction with the receptor was significantly altered compared to either native echistatin or LP-labeled echistatin. Lactoperoxidase labeling reaction seemed to preserve the binding characteristics of the native molecule.

To quantitate the dissociability of the CT-labeled echistatin, its rate of dissociation was determined under dilution conditions rather than competitive displacement. After saturation of the receptor with CT-labeled ^{125}I-echistatin, the radioligand was removed and replaced with buffer. At specific time points, the presence of ligand was quantitated both in the aqueous phase and that which was receptor associated. The dissociation rate constant was calculated from simple first-order kinetics as described by the following equation: $\ln(LR)/LR = -k_{-1}t$. As shown in Fig. 3C, the CT-labeled echistatin rapidly dissociates from the receptor into the aqueous phase with a dissociation rate of 3.7×10^{-4} s^{-1}. Previous studies have shown that vitronectin binds to integrin $\alpha_v\beta_3$ in a non-dissociable manner, whereas the binding of an RGD peptide

→

Fig. 4. Electrospray mass spectrometric analysis of the lactoperoxidase and chloramine T-treated unlabeled echistatin. The electrospray (ES) mass spectrum of echistatin was obtained by dissolving the sample in 0.1% aqueous TFA (~5 pmol/μl) and then infusing into the ion-spray source at a flow rate of 5 μl/min. The deconvoluted spectrum shown in panel A is derived from the observed charged states with the most prominent being the +4, +5 and +6 states. Similarly, the lactoperoxidase and chloramine T-treated unlabeled echistatin was chromatographed and the major chromatographic peak was isolated and subjected to ES mass spectrometric analysis. The respective deconvoluted ES mass spectra shown in panels B and C indicate that the chloramine T treatment increased the molecular weight of the peptide by 16 Da.

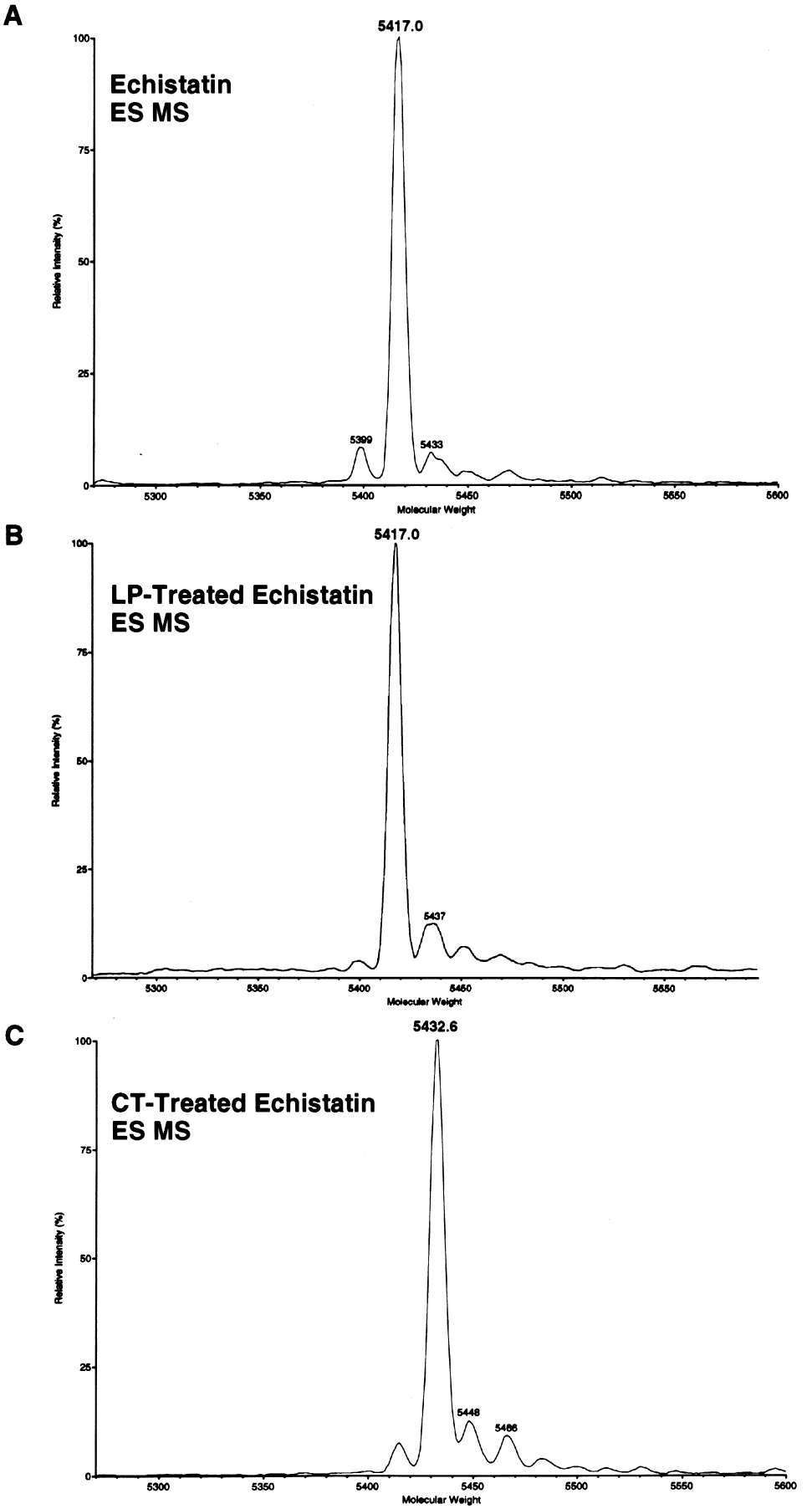
A
5417.0
Echistatin
ES MS
5399
5433
Relative Intensity (%)
Molecular Weight
B
5417.0
LP-Treated Echistatin
ES MS
5437
Relative Intensity (%)
Molecular Weight
C
5432.6
CT-Treated Echistatin
ES MS
5448
5466
Relative Intensity (%)
Molecular Weight

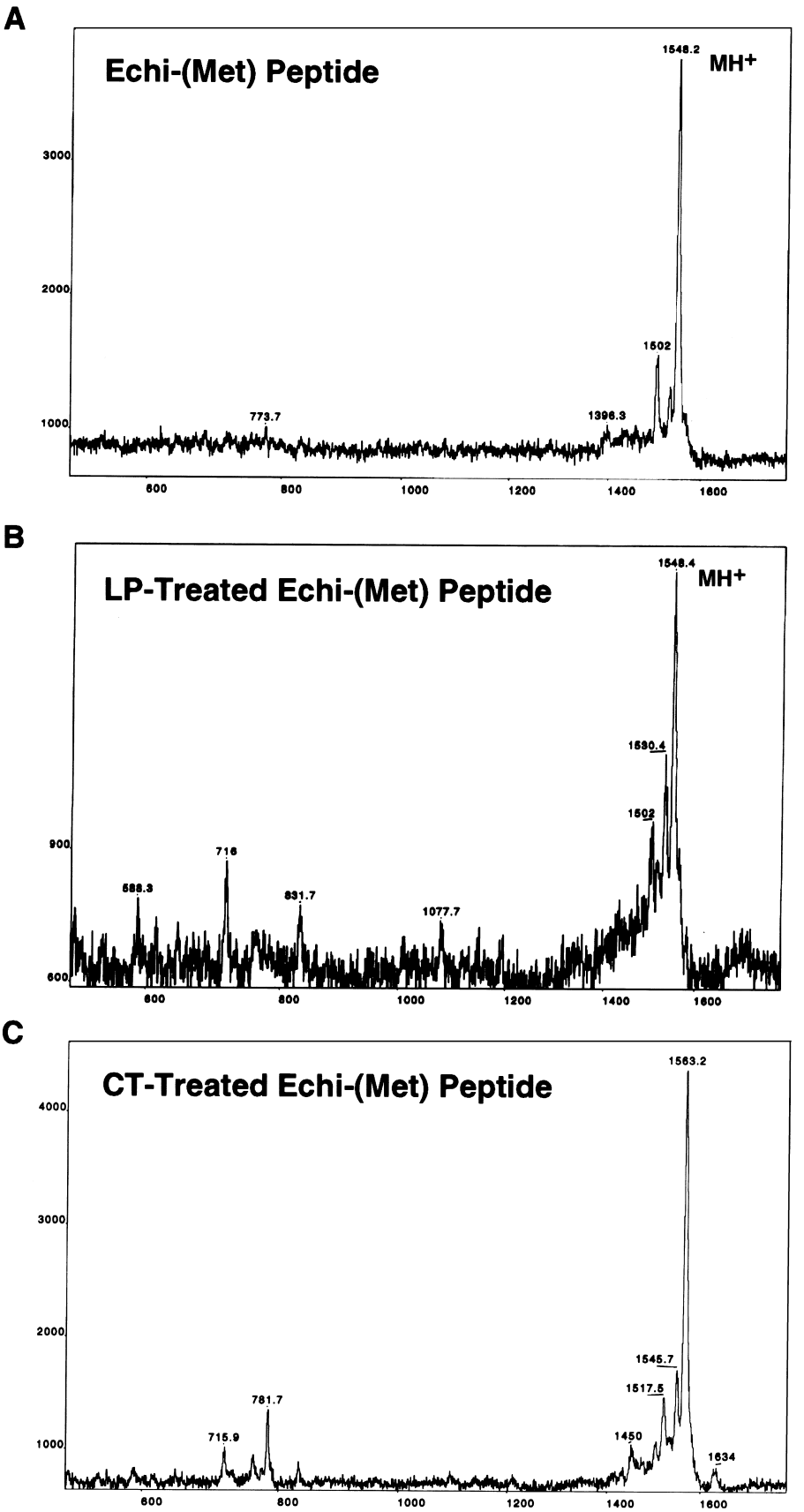
A
Echi-(Met) Peptide
1548.2
MH+
3000
2000
1000
1502
773.7
1396.3
600
800
1000
1200
1400
1600
B
LP-Treated Echi-(Met) Peptide
1548.4
MH+
1530.4
1502
900
716
588.3
831.7
1077.7
600
800
1000
1200
1400
1600
C
CT-Treated Echi-(Met) Peptide
1563.2
4000
3000
2000
1000
1545.7
1517.5
781.7
715.9
1450
1634
600
800
1000
1200
1400
1600

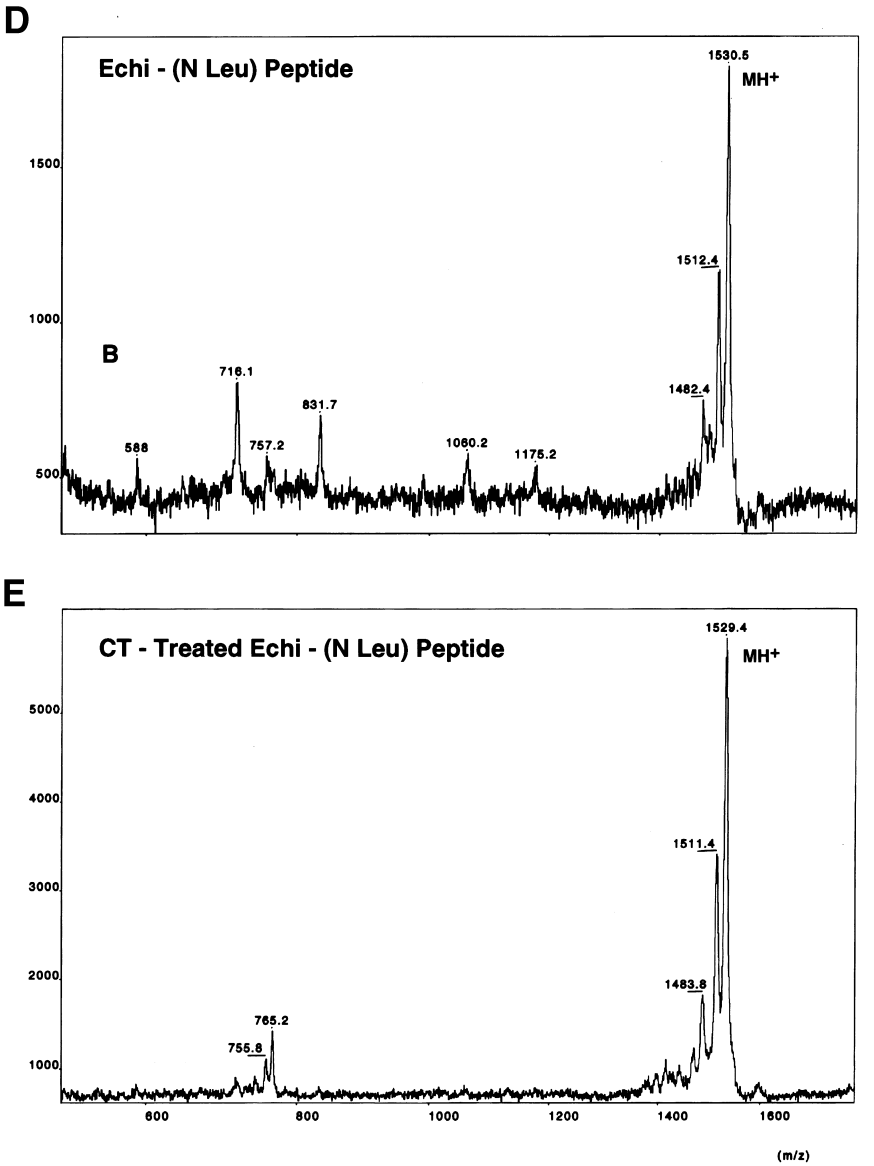

Fig. 5. Plasma desorption mass spectrometric analysis of the lactoperoxidase and chloramine T-treated echistatin (Met) and (N-Leu) peptides. The plasma desorption (PD) mass spectrum of the echistatin (Met) synthetic peptide was obtained by dissolving the sample in 2:1 (v/v) 0.1% aqueous TFA:ethanol, spin-drying and then analyzing them by PD mass spectrometry. The PD mass spectrum shown in panel A shows the protonated molecular ion (MH^+). Similarly, the lactoperoxidase and chloramine T-treated echistatin (Met) peptides were chromatographed and the major chromatographic peaks were isolated and subjected to PD mass spectrometric analysis. From the respective PD mass spectra shown in panels B and C, the chloramine T treatment induces a 16 Da increase in the molecular weight. D and E: PD mass spectrometric analysis of the lactoperoxidase and chloramine T-treated echistatin (N-leu) peptide. Echistatin (N-Leu) synthetic peptide was dissolved in 2:1 (v/v) 0.1% aqueous TFA:ethanol by spin-drying and then analyzed by PD mass spectrometry. The PD mass spectrum of the major chromatographic peak of the chloramine T-treated echistatin (N-Leu) peptide (panel E) was identical to that of the untreated echistatin (N-Leu) peptide (panel D).

derived from vitronectin is specific but is completely dissociable [18]. The interaction of $\alpha_v\beta_3$ with vitronectin involves the initial integrin-ligand recognition event, which is RGD dependent and fully dissociable, followed by stabilization of the receptor-ligand complex leading to a non-dissociable interaction between these proteins. The dissociation rate constant for ^{125}I-vitronectin-derived peptide is 1.6×10^{-4} s^{-1} and is close to the value obtained for CT-treated echistatin. These studies indicate that native and LP-labeled echistatin bind to $\alpha_v\beta_3$ in a non-dissociable manner similar to vitronectin. In contrast, CT-labeled echistatin behaves very similar to the RGD peptide derived from vitronectin.

3.3. *Chloramine T reaction leads to the oxidation of methionine residue in echistatin*

To determine if there were any major structural changes in echistatin induced by LP or CT treatment, unlabeled echistatin was subjected to LP or CT treatment in the absence of NaI^{125} and the products were analyzed by ion-spray mass spectrometry following purification of the products by HPLC [19,20]. As shown in Fig. 4A, the measured molecular mass of echistatin was 5416.5 consistent with the calculated molecular mass of 5417 assuming four disulfide bonds in the protein. Lactoperoxidase treatment of echistatin did not change the molecular mass of the protein (Fig. 4B). On the

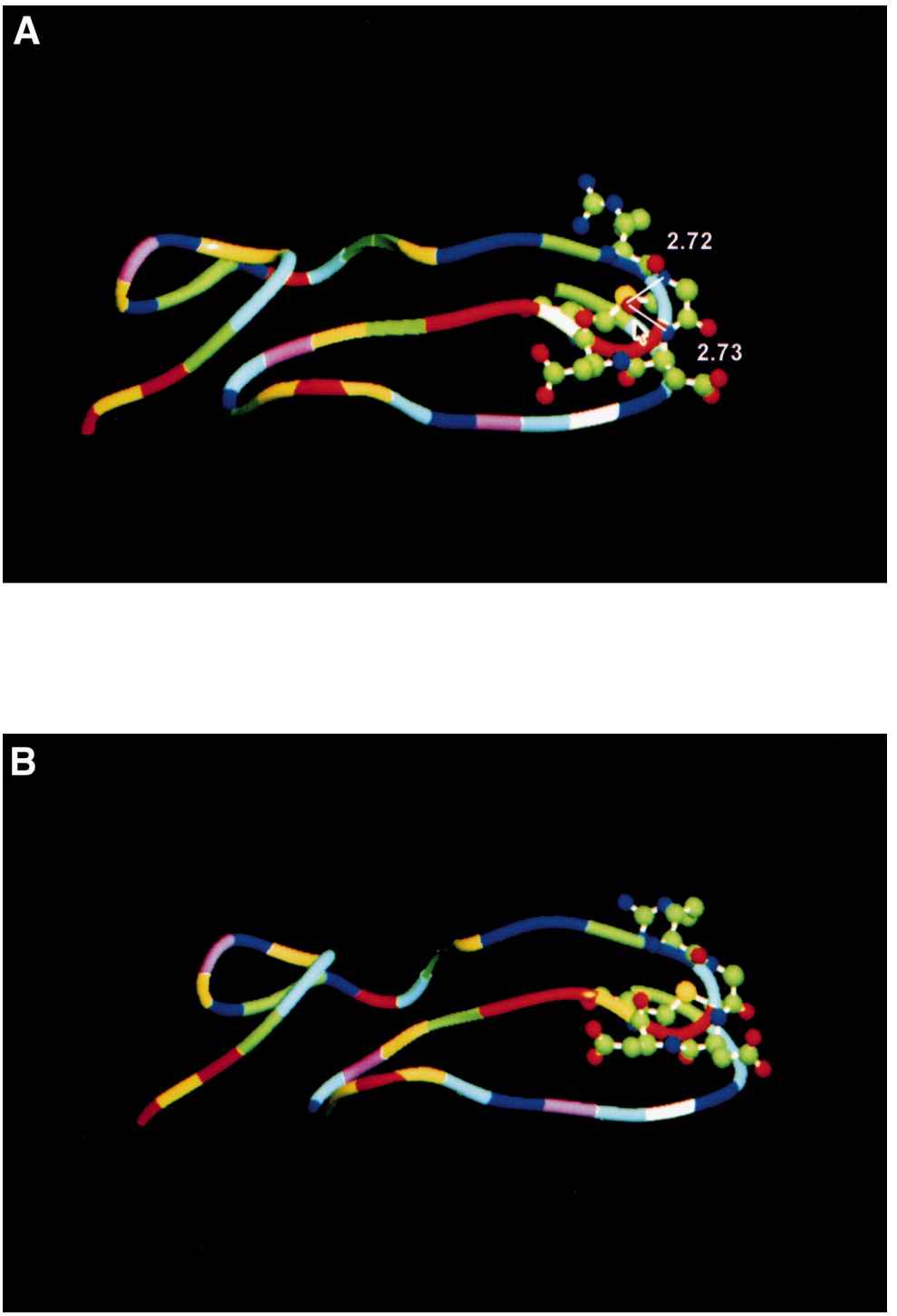

Fig. 6. Molecular structure for modified echistatin constructed using molecular dynamics simulation methods. Residue backbone and atoms are color-coded as follows: green, hydrophobic; red, positively charged; blue, negatively charged; yellow, sulphur-containing residues; pink/pale blue, hydrophilic; magenta, aspargine/glutamine; cyan, glycine/proline. the side chain atoms of amino acids RGDDM are shown in ball and stick models. A: Ribbon drawing for the structure of modified echistatin developed using molecular dynamics simulation methods is shown. The hydrogen bond distances between (Met-28) O- - -H-N (Gly-25) 2.72 Å and (Met-28) O- - -H-N (Asp-26) 2.73 Å are indicated in the figure. Residue backbone and atoms are color-coded as follows: green, hydrophobic; red, positively charged; blue, negatively charged; yellow, sulphur-containing residues; pink/pale blue, hydrophilic; magenta, aspargine/glutamine; cyan, glycine/proline. The side chain atoms of amino acids RGDDM are shown in ball and stick models. B: Ribbon representation for the structure of native echistatin with the same color-coding scheme of residues and atoms as described above.

other hand, treatment of echistatin with chloramine T increased the mass by 16 units, suggesting the addition of an extra oxygen atom to the molecule (Fig. 4C).

To identify the precise amino acid residue in echistatin that has picked up the oxygen atom, the CT-treated echistatin was subjected to tryptic digestion followed by purification of the

resulting peptides on HPLC and subjecting them to mass spectrometric analysis. Tryptic digestion of echistatin gave a complex pattern of peptides owing to the four disulfide bonds in the molecule. Hence, we used an alternate approach. It is believed that the methionine residues are susceptible to oxidation during chloramine T treatment [26]. Echistatin contains a single methionine residue close to the RGD sequence [1–3]. Hence, a 13 amino acid long synthetic peptide corresponding to the flexible RGD loop of echistatin was subjected to CT or LP treatment and analyzed by mass spectrometric analysis. As a control, we synthesized a 13 amino acid long peptide containing a single substitution of norleucine residue for methionine at position 9 in the peptide. The two peptides (Echi-Met and Echi-N Leu) were treated with LP or CT and the products were purified by HPLC before subjecting them to plasma desorption mass spectrometric analysis. As shown in Fig. 5A, the measured molecular mass of the 13 amino acid long peptide containing methionine was 1548. LP treatment of the peptide did not alter the molecular weight of the peptide (Fig. 5B). However, CT treatment of the peptide increased the mass by 16 units suggesting that this peptide containing the methionine residue has picked up an extra oxygen atom (Fig. 5C). In contrast, the peptide containing norleucine substituted for methionine did not show any change in the molecular mass following CT treatment (Fig. 5D and E). LP-treated peptide also gave identical spectra (results not shown) These results indicate that the methionine residue following the RGDD sequence is the one that picked up the oxygen atom following treatment with chloramine T.

3.4. Development of three-dimensional structure of chloramine T-labeled echistatin using homology methods

To gain insights into the structural changes induced by chloramine T treatment of echistatin and to understand the basis for the observed changes in the binding characteristics of the molecule, we have developed the molecular structure for echistatin with methionine sulfoxide as its residue 28 in the native molecule. The structure of echistatin is predominantly a loop structure with four non-standard turns. The folding forces are largely due to the four disulfide bridges between all eight cysteine residues which are highly conserved in all disintegrins. The eight cysteine residues in the protein, which are widely distributed in the sequence, are localized in one half of the molecule and the loop containing the RGD sequence and the C-terminal end is located in the other half of the molecule (shown in Fig. 6). The RGD residues form a loop at the tip of the hairpin formed by the two short irregular antiparallel strands. The C-terminal end of the protein is in the proximity of the RGD loop and appears to be most mobile. The three-dimensional structure developed for the modified echistatin using molecular dynamics simulation compared well with that of native echistatin. The model was then refined using conjugate gradient energy minimization method by Powell [19]. The energy-minimized model was further refined using a slow-cooling simulated annealing molecular dynamics procedure using X-PLOR [25]. The root-mean-square (rms) deviations in Cα coordinates between these two protein structures is 0.7 Å. The total energy calculated by considering the various interactions, such as hydrogen bonding, partial charge interactions, electrostatic, van der Waal's interactions, etc. for echistatin is −1112 kcal, and for modified echistatin is −1155 kcal. The rms deviations in Cα atoms between echistatin and echistatin with methionine sulfoxide at residues 28 is 0.7 Å. In the native structure of echistatin the methionine residue is tucked between the RGD loop and the C-terminal loop which are antiparallel to each other (shown in Fig. 6A). Although the environment of the methionine sulfoxide residue in the structure of modified echistatin is very similar to that of native molecule, the presence of oxygen atom on methionine side chain forms two strong hydrogen bonds with the main chain nitrogen atoms of residues Gly and Asp of RGD loop. The two hydrogen bonds are (Met-28) O- - -H-N (Gly-26) 2.65 Å and (Met-28) O- - -H-N (Asp-27) 2.67 Å. The formation of such strong hydrogen bonds between the side chain of methionine residue and the residues in the RGD loop constrains the conformational flexibility of the RGD loop and may contribute to the lower binding affinity of the molecule and to the dissociable nature of the interaction with $\alpha_v\beta_3$ receptor.

Acknowledgements: We wish to thank Mike Malkowski for excellent technical assistance. This work is partially supported by funds from FELS Institute for Cancer Research.

References

[1] Gan, Z.R., Gould, J.R., Jacobs, J.W., Friedman, P.A. and Polokoff, M.A. (1988) J. Biol. Chem. 263, 19827–19832.
[2] Niewiarowski, S., McLane, M.A., Kloczewiak, M. and Stewart, G.S. (1994) Sem. Hematol. 31, 289–300.
[3] Gould, R.J., Polokoff, M.A., Friedman, P.A., Huang, T.F., Holt, J.C., Cook, J.J. and Niewiarowski, S. (1990) Proc. Soc. Exp. Biol. Med. 195, 168–171.
[4] Krezel, A.M., Wagner, G., Seymour-Ulmer, J. and Lazarus, R.A. (1994) Science 264, 1944–1947.
[5] Scaloni, A., Dimartino, E., Miraglia, N., Pelagalli, A., Della Morta, R., Staiano, N. and Pucci, P. (1996) Biochem. J. 319, 775–779.
[6] McLane, M.A., Kowalska, M.A., Silver, L., Shattil, S.J. and Niewiarowski, S. (1994) Biochem. J. 301, 429–434.
[7] Saudek, V.R., Atkinson, A. and Pelton, J.T. (1991) Biochemistry 30, 7369–7372.
[8] Garsky, V.M., Lumma, P.K., Friedinger, R.M., Pitzanberger, S.M., Randall, W.C., Veber, D.F., Gould, R.J. and Friedman, P.A. (1989) Proc. Natl. Acad. Sci. USA 86, 4022–4026.
[9] Hynes, R.O. (1992) Cell 69, 11–25.
[10] Clark, A.E. and Brugge, J.S. (1995) Science 268, 233–239.
[11] Juliano, R.L. and Haskill, S. (1993) J. Cell Biol. 120, 577–585.
[12] Sastry, S.K. and Horwitz, A.F. (1993) Curr. Opin. Cell Biol. 5, 819–831.
[13] Ruoslahti, E. and Pierschbacher, M.D. (1987) Science 238, 491–497.
[14] Varner, J.A. and Cheresh, D.A. (1996) in: V.T. DeVita, S. Hellman and S.A. Rosenberg (Eds.), Important Advances in Oncology, Lippincott-Raven Publishers, Philadelphia, PA.
[15] Brooks, P.C., Montgomery, A.M.P., Rosenfeld, M., Reisfeld, R.A., Hiu, T., Klier, G. and Cheressh, D.A. (1994) Cell 79, 1157–1164.
[16] Brooks, P.C., Clark, R.A.F. and Cheresh, D.A. (1994) Science 264, 569–571.
[17] Chandra Kumar, C., Nie, H., Prorock-Rogers, C., Malkowski, M., Maxwell, E., Catino, J.J. and Armstrong, L. (1997) J. Pharmacol. Exp. Ther. 283, 843–853.
[18] Orlando, R.A. and Cheresh, D.A. (1991) J. Biol. Chem. 266, 19543–19550.
[19] Covey, T.R., Bonner, R.F., Shushan, B.I. and Henion, J.D. (1988) Rapid Commun. Mass Spectrom. 2, 249.
[20] Tsarbopoulos, A., Becker, G.W., Occolowitz, J.L. and Jardine, I. (1988) Anal. Biochem. 171, 113–123.
[21] Tsarbopoulos, A., Covey, T.R., Pramanik, B.N. and Nagabhushan, T.L. (1995) J. Mass Spectrom. 30, 1752–1763.
[22] Munson, P.J. and Rodbard, D. (1980) Anal. Biochem. 107, 220–239.

[23] Jones, T.A. (1978) J Appl. Crystallogr. 11, 268–272.
[24] Powell, M.J.D. (1977) Math. Prog. 12, 241–254.
[25] Brünger, A.T., Krukowski, A. and Erickson, J.W. (1990) Acta Cryst. A46, 585–593.
[26] Chen, Y., Huang, T., Chen, S. and Tsai, I. (1995) Biochem. J. 305, 513–520.